BIOCHEMISTRY
including biophysical chemistry & molecular biology

Article

pubs.acs.org/biochemistry

Investigating the Structural Dynamics of α-1,4-Galactosyltransferase C from *Neisseria meningitidis* by Nuclear Magnetic Resonance Spectroscopy

Patrick H. W. Chan,[†,‡] Adrienne H. Cheung,[†] Mark Okon,[†,§] Hong-Ming Chen,[§] Stephen G. Withers,[†,‡,§] and Lawrence P. McIntosh*[,†,‡,∥,§]

[†]Department of Biochemistry and Molecular Biology, University of British Columbia, Vancouver, BC V6T 1Z3, Canada
[‡]Centre for High-throughput Biology, University of British Columbia, Vancouver, BC V6T 1Z4, Canada
[§]Department of Chemistry, University of British Columbia, Vancouver, BC V6T 1Z1, Canada
[∥]Michael Smith Laboratories, University of British Columbia, Vancouver, BC V6T 1Z4, Canada

Supporting Information

ABSTRACT: *Neisseria meningitidis* α-1,4-galactosyltransferase C (LgtC) is responsible for the transfer of α-galactose from donor UDP-galactose to the lipooligosaccharide terminal acceptor lactose. Crystal structures of its substrate analogue complexes have provided key insights into the galactosyl transfer mechanism, including a hypothesized need for active site mobility. Accordingly, we have used nuclear magnetic resonance spectroscopy to probe the structural dynamics of LgtC in its apo form and with bound substrate analogues. More than the expected number of signals were observed in the methyl-TROSY spectra of apo LgtC, indicating that the protein adopts multiple conformational states. Magnetization transfer experiments showed that the predominant states, termed "a" and "b", are in equilibrium on a time scale of seconds. Their relative populations change with temperature and mutations, and only the "b" state is competent for substrate binding. For both states, relaxation dispersion studies also revealed substantial millisecond time scale motions of isoleucine side chains within and distal to the active site. Although altered, these motions were still detected in LgtC with a noncovalently bound donor analogue. A mutant, LgtC-Q189E, which forms an unexpected glycosyl−enzyme intermediate via a residue (Asp190) distal from its active site, was also investigated. Apo LgtC-Q189E did not show any enhanced motions that might account for the dramatic structural change required for the galactosylation of Asp190, yet formation of a trapped glycosyl−enzyme intermediate substantially reduced its millisecond time scale conformational mobility. Although further studies are required to link the detected motions of LgtC with its enzymatic mechanism, this work clearly demonstrates the complex structural dynamics of a model glycosyltransferase.

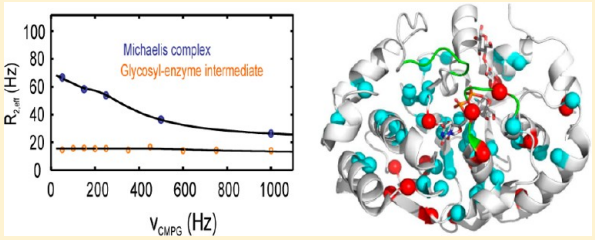

Lipooligosaccharide α-1,4-galactosyltransferase C (LgtC) is a family 8 glycosyltransferase (GT)[1] that catalyzes transfer of α-galactose from the sugar donor uridine-5′-diphosphate galactose (UDP-Gal) to a terminal lactose sugar acceptor on the cell wall lipooligosaccharide (LOS) of *Neisseria meningitidis*. This leads to the synthesis of a LOS that resembles human glycoproteins, thereby helping the common nasal commensal bacterium to evade its host's immune system.[2] The enzyme follows an ordered bi-bi mechanism, with UDP-Gal·Mn^{2+} binding before the acceptor, and yields a product with net retention of stereochemistry at the donor sugar glycosidic bond.[3] The structures of LgtC with the UDP-2-deoxy-2-fluorogalactose (UDP-2FGal) donor analogue bound in the absence (binary complex) and presence (ternary) of the acceptor analogue 4′-deoxylactose have been determined using X-ray crystallography and are essentially the same.[4] Both revealed that monomeric LgtC consists of a large N-terminal mixed α/β domain, containing the active site, and a smaller C-terminal helical domain, which mediates membrane attachment. The full sugar acceptor binding site is proposed to be formed only upon the binding of UDP-Gal·Mn^{2+}, which becomes buried by the ordering of two potentially flexible loop regions (Figure 1). Although X-ray crystallographic structural information for apo LgtC is lacking, these loops are thought to at least transiently adopt an opened conformation to allow donor binding and product release.[5] Similar phenomena have been reported in a number of other GTs, such as the sialyltransferases CstI and CstII from *Campylobacter jejuni*.[6,7]

The enzymology of LgtC has been investigated in great detail, yet aspects of its catalytic mechanism remain uncertain.[3,4,8−11] Initially, a double-displacement S_N2 (bimolecular nucleophilic substitution) mechanism, akin to that well established for retaining glycoside hydrolases, was

Received: September 27, 2012
Revised: December 21, 2012
Published: December 21, 2012

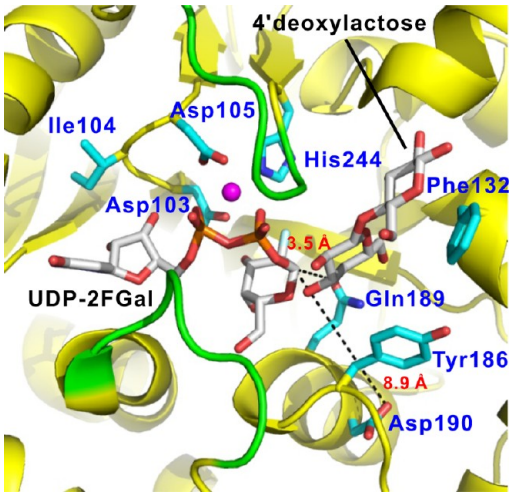

Figure 1. Expanded view of the active site of the crystal structure of the LgtC ternary complex (Protein Data Bank entry 1GA8) with bound UDP-2FGal·Mn^{2+} and 4′-deoxylactose. Side chains that interact with the substrates are shown as sticks, and the proposed flexible loops (residues 75−80 and 246−251) are colored green.

proposed for LgtC to account for the net retention of stereochemistry at the donor anomeric carbon (Figure S1 of the Supporting Information). By analogy with the hexosaminidases, the side chain amide of Gln189, which is 3.5 Å from the anomeric carbon of UDP-2FGal, was cautiously suggested as the catalytic nucleophile.[4] However, ∼3% residual activity was observed in both the Q189A and Q189E mutants of LgtC, thus bringing into question the postulated essential role of the glutamine amide.[4,10] Furthermore, whereas a covalent glycosyl−enzyme intermediate has never been detected for the wild-type enzyme, the LgtC-Q189E mutant is covalently modified with a single galactose when treated with UDP-Gal.[10] Upon addition of lactose, this trapped intermediate could be "turned over" with the same rate constant that has been observed for the transferase activity of the mutant and thus is catalytically competent. Surprisingly, the galactose was found by ESI-MS to be linked to the side chain of Asp190 and not to the anticipated Glu189. The distance between the carboxylate of Asp190 and the anomeric carbon of UDP-2FGal is ∼9 Å in the very similar crystal structures of both the wild-type and mutant enzymes complexed noncovalently with this donor analogue (Figure 1). Thus, formation of the covalent bond between Asp190 and

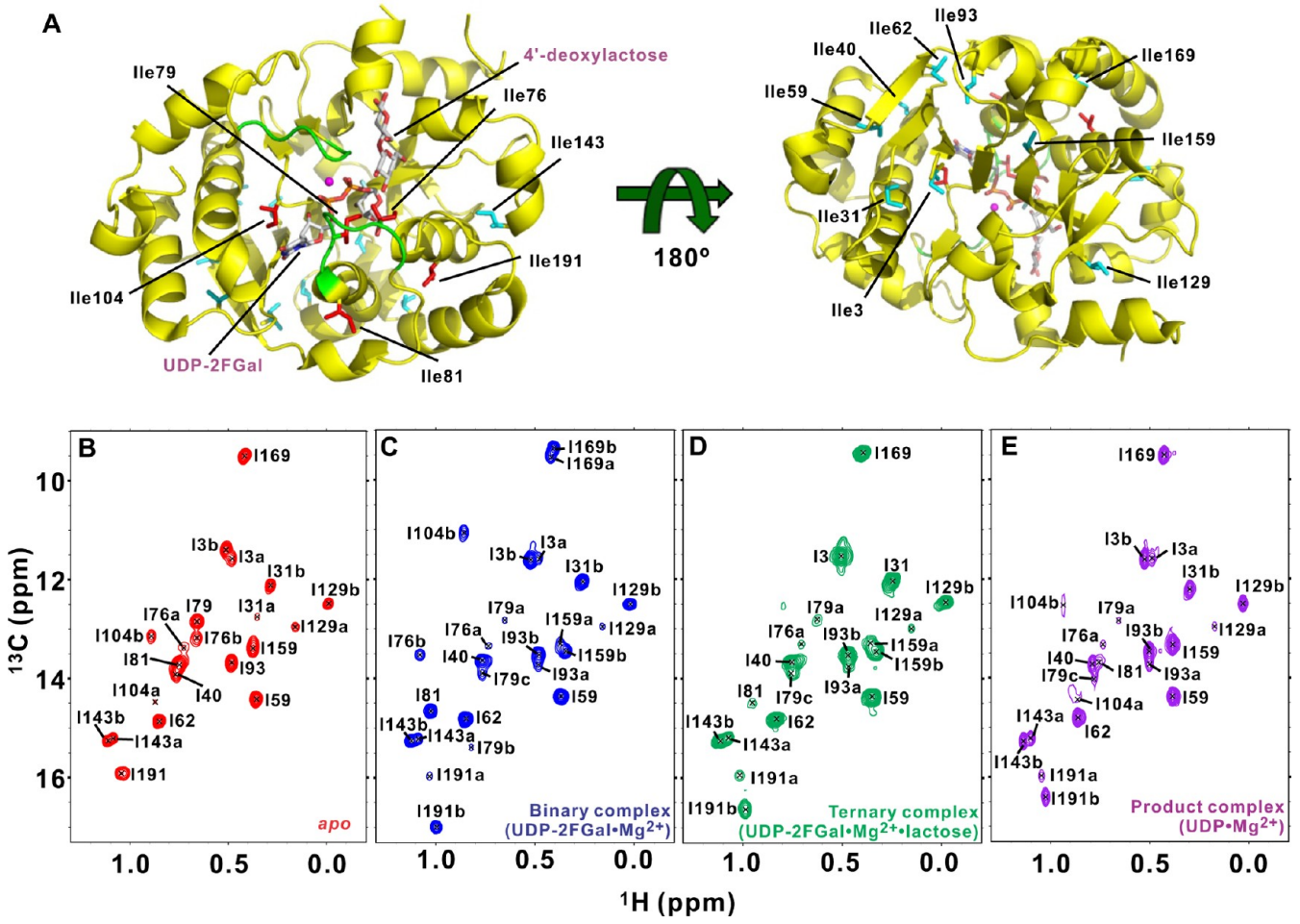

Figure 2. (A) Crystal structure of the LgtC ternary complex showing the isoleucine residues close to (red) or distal from (cyan) the active site. Ile76, Ile79, and Ile81 are within or flanking the flexible loops (green) covering the active site. Ile104 belongs to the Asp-X-Asp motif used for metal (Mn^{2+} or Mg^{2+}) binding. Ile191 is located in the α-helix that also contains Gln189 and Asp190. (B−E) methyl-TROSY spectra[18] of the isoleucine residues of the uniformly deuterated and selectively [^{1}H,^{13}C]methyl-labeled (B) apo LgtC, (C) LgtC binary complex with 10 mM Mg^{2+} and 1 mM UDP-2FGal, (D) LgtC ternary complex with 10 mM Mg^{2+}, 1 mM UDP-2FGal, and 300 mM lactose, and (E) LgtC product complex with 20 mM Mg^{2+} and 1 mM UDP were assigned previously.[16]

dx.doi.org/10.1021/bi301317d | *Biochemistry* 2013, 52, 320−332

galactose in LgtC-Q189E would require a dramatic conformational change that is not observed crystallographically. It is not at all clear whether Asp190 also plays the role of nucleophile in the wild-type enzyme or whether this is an unusual, albeit very interesting, side reaction arising because of the formation of a reactive carbocation in a potentially dynamic enzyme active site. Regardless, a covalent glycosyl−enzyme intermediate is catalytically relevant in the LgtC-Q189E mutant, and significant conformational flexibility is required in that context.

On the basis of structural considerations and the lack of an unambiguous nucleophilic residue in wild-type LgtC, an alternative S_Ni ("internal return" nucleophilic substitution) or S_Ni-like mechanism was also proposed to account for the stereochemical outcome of its transferase reaction (Figure S1 of the Supporting Information).[4,11] The latter involves a short-lived oxocarbenium ion-like intermediate that is stabilized by interactions with the UDP leaving group phosphate and undergoes a "front-side attack" by the lactose acceptor. Such a mechanism has received support from theoretical calculations,[12−14] as well as recent detailed studies of other retaining GTs.[15]

Further insights into which mechanism is more probable might be obtained by nuclear magnetic resonance (NMR) spectroscopic structural and dynamic studies of wild-type and mutant LgtC along its reaction pathway with substrate analogues, inhibitors, and trapped intermediates. As a prerequisite for these studies, we partially assigned the amide $^1H^N-^{15}N$ and methyl $^1H-^{13}C$ signals of LgtC in its apo, substrate analogue, and product complexes using complementary spectroscopic and isotope labeling approaches.[16] Although the experiments were facilitated by deuteration and amino acid selective ^{15}N labeling, we could detect only ∼70% and assign ∼50% of the expected $^1H^N-^{15}N$ signals in the ^{15}N-TROSY-HSQC spectrum of the apo enzyme. Strikingly, the assigned amides were all distal from its active site. Furthermore, although causing extensive chemical shift changes, the addition of substrate analogues did not lead to the appearance of the missing NMR signals. This observation immediately suggested that the active site of LgtC in its free and bound states exhibits backbone dynamics on microsecond to millisecond time scales that lead to $^1H^N-^{15}N$ conformational exchange broadening.[17]

In contrast, the methyl-TROSY spectra of selectively Ile/Leu/Val $^{13}CH_3$-labeled LgtC contained more than the expected number of signals, indicating that these aliphatic side chains also adopt multiple conformations. The methyl-TROSY signals from all 15 isoleucines in LgtC were assigned completely by systematically replacing each with a valine (Figure 2). Several of these residues exhibited two signals, denoted as "a" and "b". Importantly, upon titration with UDP-2FGal·Mg^{2+}, the "a" peak intensities decreased whereas the "b" peaks both shifted in frequency and increased in intensity. A simple interpretation of these results is that LgtC exists in an equilibrium between at least two predominant conformations, with substrates binding to only the one yielding the isoleucine methyl-TROSY "b" peaks. Importantly, these results suggested that the structure and dynamics of apo LgtC might differ from those observed in the static X-ray crystallographic models of its binary and ternary complexes.[4]

In this study, we demonstrate that the detected conformational states of LgtC are indeed in a temperature-dependent equilibrium and interconvert on a time scale of seconds. Layered upon this interconversion, these states also exhibit a range of faster millisecond time scale motions that can be quantified by NMR methyl relaxation dispersion methods. The addition of substrate analogues altered but did not eliminate the latter motions of the wild-type enzyme. We also determined that the Q189E mutant of LgtC does not exhibit any unusual detectable dynamic properties in its apo form, which might account for the conformational changes needed for the perplexing glycosylation of Asp190. However, relaxation dispersion approaches revealed that dynamic processes in the millisecond range are significantly dampened upon formation of the LgtC-Q189E covalent glycosyl−enzyme intermediate. Although the structural origins and functional significance of the multiple conformational states of LgtC remain to be established, our research clearly demonstrates that this enzyme exhibits a range of complex motions consistent with, but more extensive than, the simple loop closure motions previously proposed for glycosyltransferases.[11]

MATERIALS AND METHODS

Protein Expression and Purification. The plasmid encoding LgtC with the C128S, C174S, and T273A mutations, the deletion of the C-terminal 25-residue membrane association sequence, and a TEV protease-cleavable C-terminal His_6 tag has been described previously.[4,16] Additional mutations were introduced using the QuikChange site-directed mutagenesis procedure (Stratagene). LgtC samples uniformly ^{15}N-labeled or selectively labeled with Ile$^{\delta1}$-[$^1H/^{13}C$], Leu-[$^{13}CH_3$,$^{12}CD_3$], and Val-[$^{13}CH_3$,$^{12}CD_3$] in an otherwise deuterated background were expressed and purified for analysis by methyl-TROSY approaches using published protocols.[16,18,19] Saturating concentrations of 10 mM $MgCl_2$, 1 mM UDP-Gal or UDP-2FGal, and 300 mM lactose were added to form binary and ternary substrate analogue complexes. The glycosyl−enzyme intermediate of LgtC-Q189E was formed by incubation with 20 mM UDP-galactose, along with 15 units of pyruvate kinase (Sigma-Alrich) and 50 mM phosphoenolpyruvate (PEP) to remove the product UDP, and analyzed by ESI-MS.[10]

LgtC-F132X and LgtC-Y186X with the unnatural amino acids (UAAs) *p*-trifluoromethyl-phenylalanine (CF_3Phe) and *p*-[^{13}C]methoxy-phenylalanine (O$^{13}CH_3$Phe), respectively, were prepared according to published protocols.[20,21] Site-specific incorporation of UAAs required introduction of a TAG amber stop codon in place of the wild-type codon. To label the protein with CF_3Phe, we cotransformed the plasmid encoding the mutant LgtC in *Escherichia coli* BL21(λDE3) cells along with the tetracycline-selectable pDule-tfm-Phe1 plasmid encoding an engineered suppressor tRNA/aminoacyl-tRNA synthetase pair.[20] In the case of O$^{13}CH_3$Phe, the chloramphenicol-selectable pEVOL pCNP plasmid was used.[21] The bacteria were grown in 2×YT medium, with addition of 1 mM UAA at an OD_{600} of 0.3, followed by induction with 0.5 mM isopropyl β-D-1-thiogalactopyranoside (and 0.02% arabinose with pEVOL pCNP) at an OD_{600} of 0.6, and the resulting proteins were purified by published protocols.[16] CF_3Phe was purchased from JRD Fluorochemicals Ltd., and O$^{13}CH_3$Phe was synthesized in house.[21]

NMR Spectroscopy. NMR spectra were recorded on Varian Inova 600 MHz and Bruker Avance 500, 600, and 850 MHz spectrometers equipped with cryogenic probes. Unless noted otherwise, all samples (500 μM wild-type LgtC and 100 μM LgtC-Q189E) were prepared in D_2O buffer with 20 mM d_{11}-Tris and 5 mM TCEP at pH* 8.5, and data were recorded at 25 °C. Spectra were processed and analyzed using Bruker Topspin 3.0, NMRPipe,[22] and SPARKY 3.[23] ^1H and ^{13}C

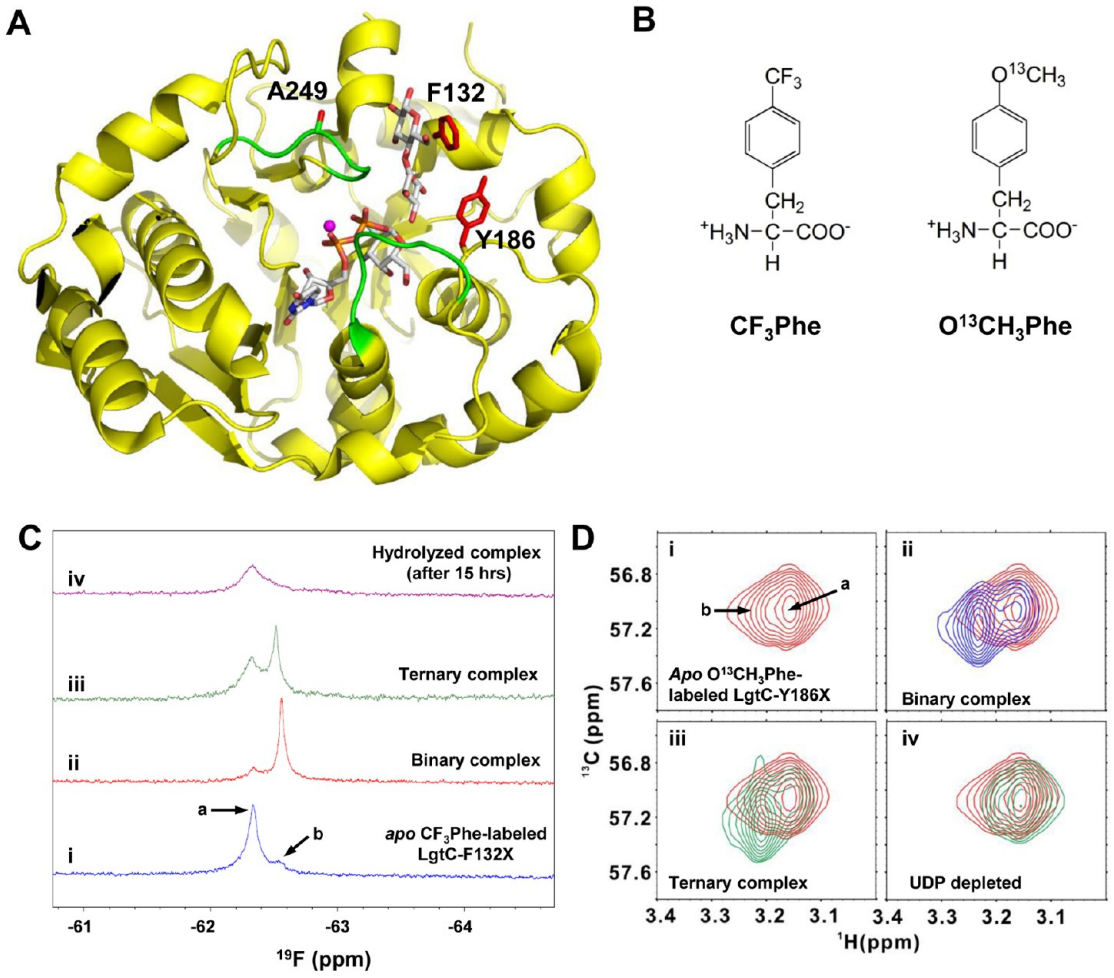

Figure 3. Two NMR-active UAAs confirm that LgtC adopts multiple conformations. (A) Phe132, Tyr186, and Ala249 are colored red in the LgtC ternary crystal structure, with active site loops colored green. Phe132 and Tyr186 interact with 4′-deoxylactose, and Ala249 is in one of the flexible loops. (B) Phe132, Tyr186, and Ala249 were replaced by the UAA CF_3Phe. Tyr186 was also replaced by $O^{13}CH_3$Phe. (C) Substrate binding by CF_3Phe-labeled LgtC-F132X was monitored using ^{19}F-NMR spectroscopy at 25 °C. Shown are spectra of (i) apo LgtC-F132X, (ii) its binary complex with 10 mM Mg^{2+} and 1 mM UDP-2FGal, (iii) its ternary complex with 10 mM Mg^{2+}, 1 mM UDP-2FGal, and 100 mM lactose, and (iv) the hydrolyzed sample after 15 h. (D) Substrate binding by $O^{13}CH_3$Phe-labeled LgtC-Y186X was monitored via ^{13}C-HSQC NMR spectroscopy at 25 °C. Shown are spectra of (i) apo LgtC-Y186X (red), (ii) its binary complex with UDP-galactose·Mg^{2+} (blue), (iii) its ternary complex with UDP-galactose·Mg^{2+}·lactose (green), and (iv) the latter sample after addition of 5 mM phosphoenolpyruvate and 10 units of pyruvate kinase to eliminate the UDP product (green). The superimposed spectrum of the apo protein is included in parts ii–iv to illustrate the chemical shift perturbations. Spectra of CF_3Phe-labeled LgtC-Y186X and LgtC-A249X are provided in Figure S4 of the Supporting Information.

chemical shifts were referenced to external 4,4-dimethyl-4-silapentane-1-sulfonic acid (DSS) and ^{19}F chemical shifts to external trifluoroacetic acid (TFA) at −76.5 ppm (relative to trichlorofluoromethane at 0 ppm).

Conformational exchange in LgtC on a time scale of seconds was measured using a pulse sequence to detect transfer of methyl H_zC_z two-spin longitudinal coherence with read-out in the form of a methyl-TROSY spectrum (Figure S2 of the Supporting Information).[24,25] Exchange rate constants were obtained by fitting the resulting time-dependent data, extracted using the nlinLS routine of NMRPipe,[22] to published equations[26] with GraphPad Prism. Details of the analysis are provided in Figure S3 of the Supporting Information. In the case of CF_3Phe-labeled LgtC-F132X, conformational exchange was detected qualitatively using a ^{19}F-NOESY pulse sequence.

Faster microsecond to millisecond time scale conformational exchange was measured with 600 and 850 MHz spectrometers using a CPMG-based multiple-quantum methyl-TROSY relaxation dispersion experiment.[27] Spectra were recorded in an interleaved (or pseudo-three-dimensional) mode with a constant time delay of 20 ms and ν_{CPMG} values ranging from 50 to 1000 Hz. The resulting dispersion curves were generated using the nlinLS routine of NMRPipe[22] to obtain values of the effective transverse relaxation rate $R_{2,eff} = (-1/T)\ln(I_{CPMG}/I_o)$ as a function of ν_{CPMG}, where I_{CPMG} and I_o are fit Gaussian peak heights with and without the CPMG pulse train, respectively. The standard deviations of the $R_{2,eff}$ values were obtained either from complete repeat measurements on two different sample of apo LgtC, from three repeat points at all five ν_{CPMG} values used for the binary complex of LgtC with UDP-2FGal·Mg^{2+}, or from two repeat points at one intermediate ν_{CPMG} for LgtC-Q189E in its apo and trapped glycosyl–enzyme intermediate states. Conformational exchange rate constants for apo wild-type LgtC were extracted by global fitting to a two-state model with the analysis program GUARDD and errors obtained via a Monte Carlo approach.[28]

Structural Analyses and Molecular Graphics. PyMol was used to render structural figures of the LgtC ternary

dx.doi.org/10.1021/bi301317d | *Biochemistry* 2013, 52, 320–332

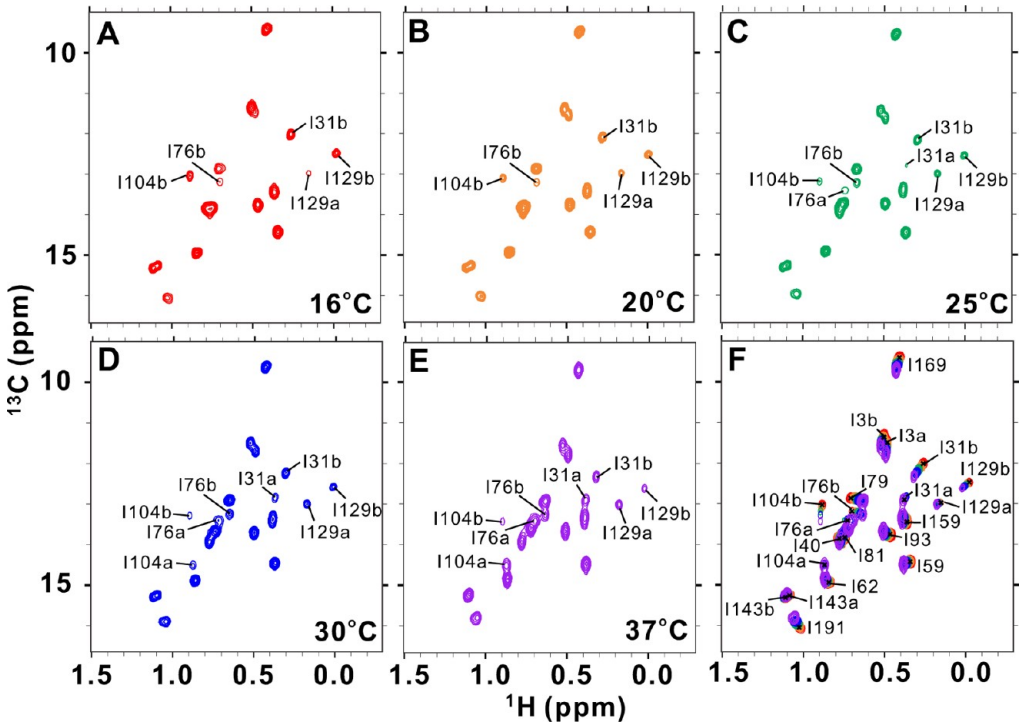

Figure 4. Apo LgtC exists in a conformational equilibrium with the state leading to the "a" peaks favored at higher temperatures. Methyl-TROSY spectra of uniformly deuterated and selectively [^{1}H,^{13}C]methyl-labeled LgtC were acquired as a function of temperature in random order: (A) 16, (B) 20, (C) 25, (D) 30, and (E) 37 °C. The contour levels of the spectra were adjusted by eye to compensate for temperature-dependent peak intensities and aggregation of the protein. In addition to the small progressive chemical shift changes seen in the overlaid spectra (F), the relative intensities of the "a" vs "b" peaks for several isoleucines increased with increasing temperature. For the sake of clarity, only selected peaks are labeled in panels A–E.

complex (Protein Data Bank entry 1GA8) with UDP-2FGal·Mn^{2+} and 4′-deoxylactose shown only as appropriate. Unless noted otherwise, atoms are colored as follows: gray for carbon, red for oxygen, blue for nitrogen, orange for phosphorus, and magenta for Mn^{2+}.

RESULTS

Multiple Conformational States of LgtC Confirmed with UAAs. Our previous NMR spectroscopic studies of LgtC revealed probable conformational exchange broadening of the amide $^{1}H^{N}$–^{15}N signals and multiple conformational states of the methyl groups of Ile, Leu, and Val in LgtC.[16] To test whether additional side chains also exhibit such behavior, we incorporated two NMR-active unnatural amino acid (UAA) analogues of phenylalanine into LgtC using engineered suppressor tRNA/aminoacyl-tRNA synthetases (Figure 3A,B). These noncanonical amino acids serve as unique, site-specific spectroscopic and chemical probes for studying protein structure, dynamics, and function.[29,30] Using published methods, CF_3Phe was substituted for Phe132, Tyr186, and Ala249, and O$^{13}CH_3$Phe was substituted for Tyr186. These specific residues were chosen to be minimally perturbing because of their relatively exposed positions near the active site of the enzyme. Indeed, kinetic analyses confirmed that the presence of either UAA at position 132 did not adversely affect the enzymatic activity of LgtC (Table S1 of the Supporting Information).

The ^{19}F-NMR spectra of CF_3Phe-labeled LgtC-F132X are shown in Figure 3C. In the spectrum of the apo protein, a major peak "a" and a minor peak "b" were observed. When UDP-2FGal·Mg^{2+} was added, the relative intensities of the peaks switched, consistent with peak "b" arising from a conformation resembling that of the donor-bound state. Note that position 132 is not immediately adjacent to the bound UDP-2FGal·Mg^{2+} and thus CF_3Phe132 likely reports a conformational change, rather than a direct perturbation from the donor analogue. Also, as observed previously, UDP-2FGal·Mg^{2+} binding occurred in the slow exchange limit on the ^{19}F chemical shift time scale (not shown). Addition of 100 mM lactose caused a small shift of peak "b", possibly because of a direct interaction of residue 132 and the bound acceptor. After ∼15 h, the UDP-2FGal was hydrolyzed and/or transferred to lactose and a broad signal with the chemical shift of peak "a" was observed. This presumably arises from the product complex with bound UDP, placing CF_3Phe132 in a comparable environment as with apo LgtC. The large line width of the signal is likely due to Mg^{2+}-induced aggregation of LgtC. Similar behavior, albeit with different relative "a" versus "b" peak intensity ratios, was observed in the ^{19}F-NMR spectra of CF_3Phe-labeled LgtC-Y186X and LgtC-A249X (Figure S4 of the Supporting Information), thus confirming that several side chains throughout LgtC also report at least two conformations.

In a complementary study, the ^{13}C-HSQC spectra of O$^{13}CH_3$Phe186-labeled LgtC-Y186X were recorded (Figure 3D). Initially, a major peak from O$^{13}CH_3$Phe186 with a small shoulder was observed for the apo enzyme. When the natural sugar donor UDP-Gal was added, the main peak was shifted to the position of the shoulder and a residual signal from the apo enzyme remained. Again, this is indicative of major "a" and "b" conformational states, with state "b" resembling the substrate-bound state. When lactose was added to the binary complex, the signals remained unchanged, even after 24 h. However,

dx.doi.org/10.1021/bi301317d | *Biochemistry* 2013, 52, 320–332

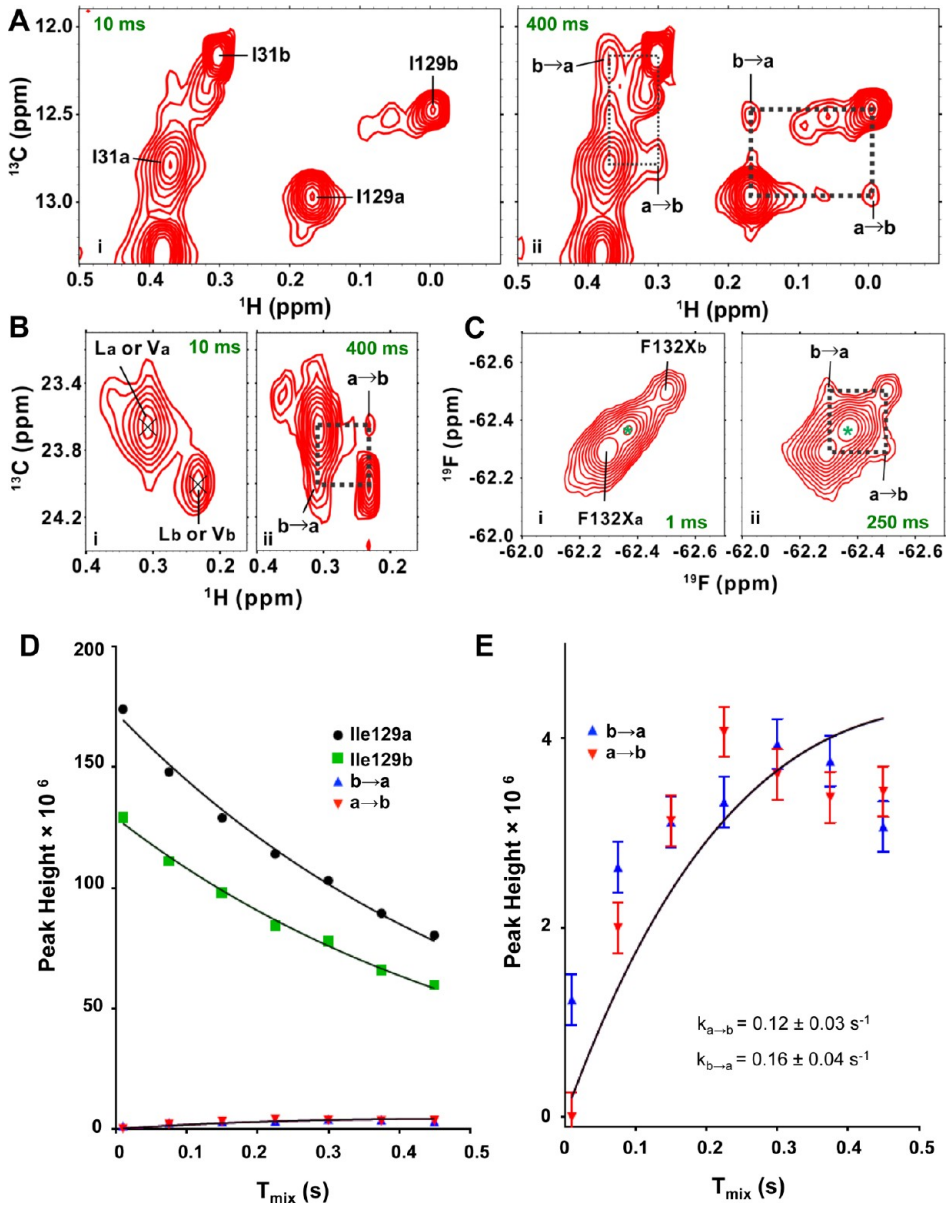

Figure 5. Magnetization exchange experiments reveal the slow interconversion between conformational states of apo LgtC at 25 °C. Exchange cross-peaks were detected in the form of methyl-TROSY spectra for (A) Ile129 and Ile31 and (B) a pair of unassigned leucines/valines. Panels i show spectra with a 10 ms transfer delay, and panels ii show spectra with a 400 ms transfer delay. (C) Exchange was also detected for CF_3Phe-labeled LgtC-F132X using a ^{19}F-NOESY experiment with (i) 1 or (ii) 250 ms transfer times. The additional diagonal signal (asterisk) was not present in the initial spectra recorded with fresh protein and is attributed to sample degradation. (D and E) The conformational exchange rate constants for Ile129 were extracted by fitting the time-dependent heights of the auto and exchange peaks, as described in detail in Figures S2 and S3 of the Supporting Information. The root-mean-square errors of the peak heights are smaller than the symbols in panel D. Panel E is an expanded view showing the "a → b" and "b → a" exchange peaks, for which the best-fit curves overlap. The modest agreement of the fit curves with the data points reflects the relatively slow conformational exchange and hence weak exchange peaks for Ile129. Because of limited spectral dispersion, it was not possible to reliably analyze the exchange data for the other residues shown in panels A–C.

when pyruvate kinase and phosphoenolpyruvate were added to deplete the product UDP, the main peak shifted back to the original chemical shifts of the apo form. Thus, it appears that O^{13}CH$_3$Phe186 has the same chemical shift when either UDP-Gal and lactose or UDP is bound or that the natural substrate was hydrolyzed rapidly to UDP. Regardless, these data confirm further that LgtC adopts multiple conformational states.

Temperature-Dependent Conformational Equilibria of LgtC. A consistent observation from the NMR spectra of the amides and methyls of LgtC, as well as from incorporated UAAs, is that many residues in the apo enzyme give two signals, denoted as "a" and "b". Although this could be due to sample heterogeneity, such as degraded or chemically modified forms of LgtC, we disfavor this possibility as the protein appears to be sufficiently pure and the multiple signals are detected in all samples of the wild-type and mutant enzymes. Furthermore, substrate binding shifts the relative ratios of the "a" and "b" peaks. Thus, we hypothesize that apo LgtC adopts at least two conformations, with "b" peaks arising from a state similar to that of its binary and ternary complexes. The presence of residual "a" peaks in spectra of the substrate-bound enzyme could arise from incomplete saturation.

dx.doi.org/10.1021/bi301317d | *Biochemistry* 2013, 52, 320–332

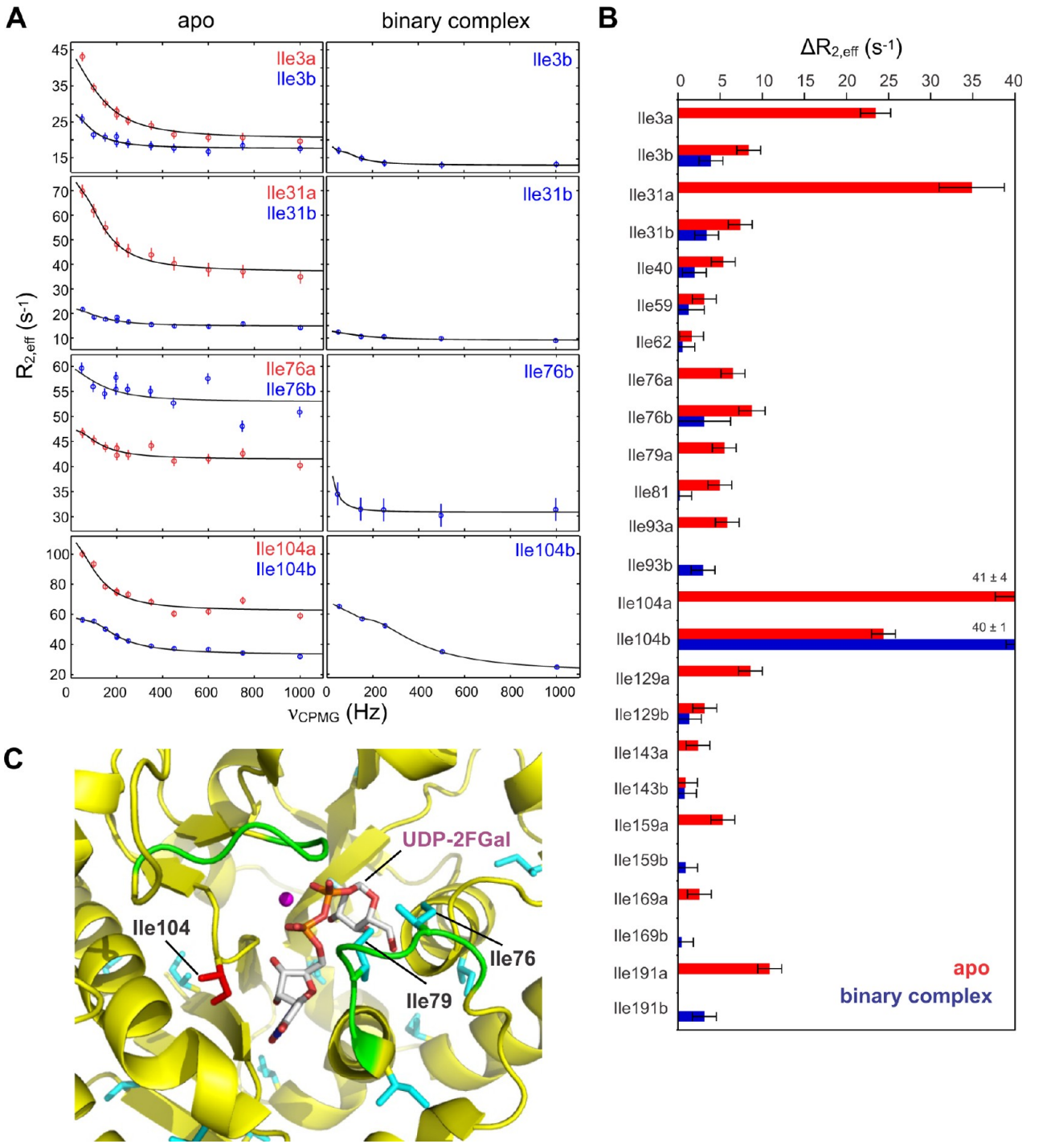

Figure 6. Methyl relaxation dispersion studies of apo LgtC and its binary complex reveal millisecond time scale conformational exchange. (A) Complete relaxation dispersion profiles of states "a" (red) and "b" (blue) recorded with a 600 MHz spectrometer for selected isoleucines of LgtC in its apo form (left) and binary complex with UDP-2FGal·Mg^{2+} (right). Error bars are standard deviations of replica data, and the lines are best fits to a two-state exchange model using GUARDD.[28] (B) Histogram showing the experimental $\Delta R_{2,\mathrm{eff}} = R_{2,\mathrm{eff}}(\nu_{\mathrm{CPMG\ 50\ Hz}}) - R_{2,\mathrm{eff}}(\nu_{\mathrm{CPMG\ 1000\ Hz}})$ values for apo LgtC (red) and its binary complex with UDP-2FGal·Mg^{2+} (blue) obtained using a 600 MHz spectrometer. The numbers are the $\Delta R_{2,\mathrm{eff}}$ values for residues with clipped histogram bars. Blanks indicate the absence of "a" signals in the binary complex or peaks with insufficient signal-to-noise ratios for reliable analysis. (C) In the structure of the LgtC binary complex, Ile104 with the largest $\Delta R_{2,\mathrm{eff}}$ values is colored red and the remaining active site isoleucines are colored cyan. The active site loops are colored green.

A key aspect of this hypothesis is that the conformational states of LgtC are in equilibrium and interconvert in the absence of substrate. To test this prediction, we recorded the methyl-TROSY spectra of apo LgtC as a function of temperature (Figure 4). Importantly, the ratio of relative intensities of the "a" versus "b" peaks for each isoleucine increased with temperature. This is consistent with a conformational equilibrium and indicates that the "a" state is favored at higher temperatures. It is also notable that these isoleucine residues are located both near (e.g., Ile76, Ile79, and Ile104,

dx.doi.org/10.1021/bi301317d | *Biochemistry* 2013, 52, 320−332

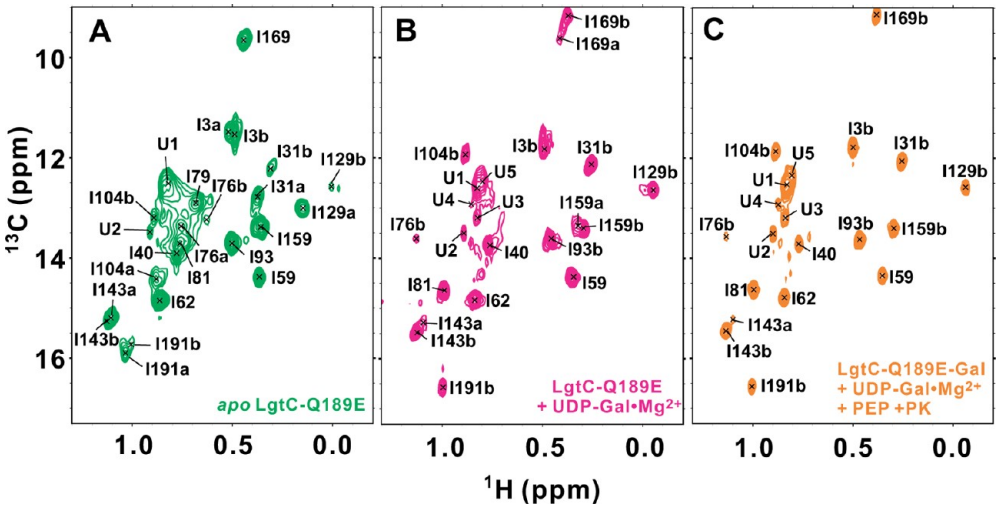

Figure 7. Methyl-TROSY spectra of the LgtC-Q189E mutant in its (A) apo form, (B) binary complex with 20 mM UDP-Gal and 10 mM Mg^{2+}, and (C) covalent glycosyl−enzyme intermediate LgtC-Q189E-Gal. Because hydrolysis of the natural substrate might occur with LgtC-Q189E, the reaction mixture was incubated for only 10 min before acquisition of panel B. The LgtC-Q189E-Gal intermediate was enriched using 50 mM phosphoenolpyruvate (PEP) and 15 units of pyruvate kinase (PK) to deplete product UDP. ESI-MS indicated that the apo enzyme and binary complex may also contain some covalent glycosyl−enzyme intermediate, whereas only a single population of modified species is observed in the presence of coupling enzyme (Figure S7 of the Supporting Information). The spectra were assigned on the basis of comparisons with those of the wild-type protein, and unassigned peaks are denoted with a U.

each of which is within 5 Å of the bound substrate) and far from (e.g., Ile31, Ile129, and Ile143, each of which is >11 Å from the bound substrate) the active site of LgtC. Thus, the conformational equilibrium is a global, rather than local, property of the enzyme.

Slow Conformational Exchange Monitored by Magnetization Transfer. Magnetization transfer experiments were also employed to detect slow exchange between the two major conformational states of apo LgtC. As shown in panels A and B of Figure 5, weak exchange cross-peaks were observed for the methyls of Ile31, Ile129, and an unassigned leucine/valine. Other residues exhibiting "a" and "b" signals did not show clear exchange peaks because of either insufficient spectral dispersion or low signal intensities after the long transfer delays. Similar weak magnetization transfer was observed in the ^{19}F-NOESY spectrum of CF_3Phe-labeled LgtC-F132X (Figure 5C). These qualitative observations confirm that apo LgtC exists as an equilibrium mixture of at least two interconverting conformational states that give rise to the "a" and "b" peaks of both the methyl groups and a UAA.

The kinetics of interconversion between the "a" and "b" states of Ile129 in apo LgtC were determined quantitatively by fitting the time-dependent intensities of its auto and exchange peaks (Figure 5D,E). At pH* 8.5 and 25 °C, the exchange rate constants for transfer from the "a" to "b" state ($k_{a\rightarrow b}$) and from the "b" to "a" state ($k_{b\rightarrow a}$) were 0.12 ± 0.03 and 0.16 ± 0.04 s^{-1}, respectively. Most importantly, these exchange rates are significantly slower than catalysis [k_{cat} = 46 s^{-1} (Table S1 of the Supporting Information)], suggesting these motions on the time scale of seconds are not directly related to or required for the enzymatic mechanism or that these processes are considerably accelerated upon binding of substrate.

Relaxation Dispersion Measurements Reveal Millisecond Time Scale Structural Dynamics in Wild-Type LgtC. Relaxation dispersion experiments were used to further investigate the dynamics of LgtC. These experiments detect the contributions of microsecond to millisecond time scale conformational exchange to the decay of transverse NMR signals.[17,31] TROSY-based methyl relaxation dispersion measurements were recorded for selectively [^{1}H,^{13}C]isoleucine-labeled deuterated LgtC using 600 MHz (Figure 6A) and 850 MHz NMR spectrometers. As seen from the resulting dispersion curves, conformational exchange is manifest as a decrease in the effective relaxation rate ($R_{2,eff}$) with an increasing refocusing pulse frequency (ν_{CPMG}). Although not shown, the effect also increases with an increasing magnetic field strength. An estimation of the exchange contribution to transverse relaxation, R_{ex}, is provided by the difference in $R_{2,eff}$ values between data collected with ν_{CPMG} values of 50 and 1000 Hz (Figure 6B).

The observation of $\Delta R_{2,eff}$ terms for many methyls in the "a" and "b" states of apo LgtC clearly reveals that both forms of the protein undergo microsecond to millisecond time scale motions. In particular, active site residues Ile76, Ile79, and, most dramatically, Ile104 exhibited methyl relaxation dispersion. However, Ile3, Ile31, and, to a lesser extent, Ile129 and Ile191 also showed conformational exchange broadening, and these residues are distal from the active site. Thus, motions extend throughout the protein scaffold. It is also noteworthy that the "a" peaks of apo LgtC showed greater exchange broadening than did the corresponding "b" peaks, suggesting that the slowly interconverting states also differ in their faster time scale dynamics. However, R_{ex} (and $\Delta R_{2,eff}$) depends not only upon the interconversion rate constant (k_{ex}) between conformational states but also upon the relative populations of those states and the magnitudes of the associated chemical shift changes ($\Delta\omega$).[17] Thus, even for a common two-state equilibrium, various reporter residues may show different $\Delta R_{2,eff}$ terms because of differential chemical shift perturbations. Indeed, global fitting of the dispersion curves for Ile3, Ile31, Ile76, Ile104, and Ile129 recorded at two magnetic fields yielded similar k_{ex} values of 880 ± 40 and 780 ± 80 s^{-1} for the "a" and "b" states, respectively. On the basis of field-dependent measurements, these dispersion curves approach the fast

dx.doi.org/10.1021/bi301317d | Biochemistry 2013, 52, 320−332

exchange limit, thus precluding a reliable estimate of the associated populations of the interconverting conformations and their chemical shift differences.[28] Nevertheless, given that these exchange rate constants are greater than the k_{cat} value of LgtC [46 s^{-1} (Table S1 of the Supporting Information)], it is tempting to speculate that these millisecond time scale motions may be a prerequisite for establishing the catalytically competent conformation of the enzyme. However, we must stress that, just as with the slowly interconverting "a" and "b" states, the structural differences associated with these millisecond transitions are currently unknown.

To investigate possible dynamic changes of LgtC upon substrate binding, methyl relaxation dispersion experiments were conducted with its binary complex with UDP-2FGal·Mg^{2+} (Figure 6). Unfortunately, because Mg^{2+} promotes LgtC aggregation and because the sugar donor analogue is hydrolyzed slowly by the enzyme, a limited data set could only be recorded at one magnetic field (600 MHz spectrometer) and with five different ν_{CPMG} values, thus precluding rigorous data analysis. Nevertheless, relaxation dispersion was also observed for many isoleucine methyls in the binary complex. The $\Delta R_{2,eff}$ terms were generally a little smaller than observed for the corresponding "b" state methyls in apo LgtC, indicating that the bound UDP-2FGal·Mg^{2+} may dampen, but not totally sequester, the millisecond time scale motions of LgtC. However, this could also reflect smaller chemical shift changes between interconverting states, rather than differences in exchange rate constants or populations. Regardless, the "b" peak from Ile104 showed substantial exchange broadening, clearly revealing that the active site of LgtC is still dynamic even with the sugar donor bound (Figure 6C).

NMR Spectroscopic Characterization of LgtC-Q189E. To provide insights into the solution structure and dynamic properties of the Q189E mutant and its covalent glycosyl−enzyme intermediate formed upon UDP-Gal addition,[10] a series of NMR experiments were also performed upon this system. ^{15}N-TROSY-HSQC and methyl-TROSY spectra of LgtC-Q189E were recorded and compared with those of the wild-type enzyme. Inspection of the overlaid ^{15}N-TROSY-HSQC spectra reveals many chemical shift perturbations as a consequence of this single mutation in the active site, indicating somewhat different structural environments (Figure S5 of the Supporting Information). The methyl-TROSY spectra, however, are more similar to each other. This allowed the assignments of the signals from isoleucine δ1-methyl groups in the spectra of the wild-type enzyme to be directly transferred to those of the mutant (Figure 7A and Figure S6 of the Supporting Information). One interesting observation is that the ratios of "a" to "b" peak intensities in the spectra of the mutant are larger than in those of the wild-type enzyme. In addition, Ile191 is split into two signals in the spectrum of apo LgtC-Q189E and two extra unassigned peaks (U1 and U2) are seen (Figure 7A). These data together suggest that the apo structures of the wild-type enzyme and the Q189E mutant in solution may be somewhat different. Presumably, the nearly identical X-ray crystallographic structures of the two proteins with UDP-2FGal·Mn^{2+} bound reflect crystal packing constraints and/or the high sensitivity of chemical shifts to even subtle structural perturbations.

Methyl-TROSY spectra of complexes of wild-type LgtC with UDP-2FGal·Mg^{2+} and LgtC-Q189E with UDP-Gal·Mg^{2+} were also compared (Figure 7B and Figure S6 of the Supporting Information). The overlaid spectra of the binary complexes reveal a greater number of chemical shift perturbations versus the number seen with the apo forms. These differences could reflect the slight physicochemical differences between UDP-Gal and UDP-2FGal. However, this seems unlikely because the fluorine points away from all the isoleucine residues in LgtC. More probable is the fact that it reflects structural differences between the wild-type and mutant enzymes, combined with the partial formation of a covalent glycosyl−enzyme intermediate, denoted as LgtC-Q189E-Gal. To more completely form LgtC-Q189E-Gal, pyruvate kinase (PK) and phosphoenolpyruvate (PEP) were added to deplete any product UDP and thereby "pull" the equilibrium fully over to the glycosyl−enzyme species. Indeed, the residual "a" peaks in the binary complex totally disappeared, indicating the formation of a single species (Figure 7C and Figure S6 of the Supporting Information), which fortunately was stable against hydrolysis as evidenced by its invariant NMR spectra recorded over several days (not shown). Parallel ESI-MS analysis of ^{15}N-labeled LgtC-Q189E (Figure S7 of the Supporting Information) also confirmed the complete conversion of the enzyme to its galactosylated form in the presence of UDP-Gal and the coupling system, as seen previously.[10] Surprisingly, ESI-MS also shows that under the conditions employed here, a fraction of the apo enzyme already bears a galactosyl moiety (Figure S7 of the Supporting Information). This presumably reflects reaction with endogenous UDP-Gal in the bacterial cells used for protein production and might account for the additional, unassigned broad peaks observed in the methyl-TROSY spectrum of apo LgtC-Q189E (Figure 7A).

Relaxation Dispersion Measurements of LgtC-Q189E. The motions of the LgtC-Q189E mutant were also examined by methyl relaxation dispersion methods. As summarized in Figure 8, the millisecond time scale dynamic behavior of apo LgtC-Q189E, as reflected by $\Delta R_{2,eff}$ terms, is approximately similar to that of the wild-type apo enzyme. One exception is the "a" peak Ile104, which shows a somewhat smaller $\Delta R_{2,eff}$ in the mutant. Regardless, substitution of Gln189 with Glu does not dramatically alter the motions of apo LgtC on this time scale. In contrast, a clear reduction in conformational exchange broadening is observed for the covalent−glycosyl enzyme intermediate LgtC-Q189E-Gal formed after addition of UDP-Gal and depletion of product UDP to generate the covalent−glycosyl enzyme intermediate LgtC-Q189E-Gal (Figure 8). This is most evident for the "b" peak of Ile104, which no longer shows any relaxation dispersion. Therefore, covalent modification of Asp190 dampens the detectable motions of the mutant enzyme.

DISCUSSION

LgtC Exists in Multiple Conformations. A synthesis of the considerable volume of NMR spectroscopic data assembled on LgtC reveals a dynamic enzyme existing in multiple conformations, of which two appear to dominate. These principal conformational states are observed as "a" and "b" peaks for numerous individual residues in backbone amide ^{15}N-TROSY-HSQC and side chain methyl-TROSY spectra,[16] as well as in spectra of LgtC variants with CF_3Phe or $O^{13}CH_3$Phe introduced as site-specific UAA probes. These peaks are clearly shown to represent spectroscopically distinct interconverting forms of LgtC by the fact that a reduction in temperature or level of binding of the substrate analogue UDP-2FGal·Mg^{2+} changes the ratio of "a" to "b" peaks in favor of the latter. Thus, the "b" conformation both corresponds to that which can bind

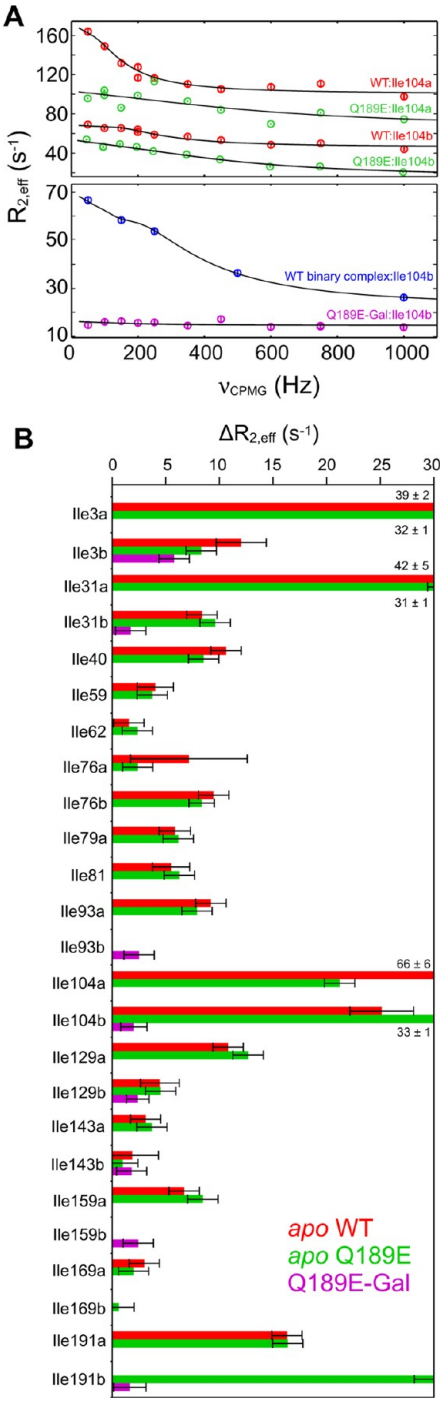

Figure 8. Methyl relaxation dispersion studies of LgtC-Q189E reveal millisecond time scale conformational exchange that is dampened upon formation of the covalent glycosyl−enzyme intermediate, LgtC-Q189E-Gal. (A) Complete 600 MHz relaxation dispersion profiles (top) of Ile104 in the "a" and "b" states of apo wild-type LgtC (red) and the "a" and "b" states of apo LgtC-Q189E (green). (A) Relaxation dispersion profiles (bottom) of state "b" of the wild-type binary complex with UDP-2FGal·Mg^{2+} (blue) and the covalently modified LgtC-Q189E-Gal (magenta). Error bars are smaller than the symbols, and the lines are best fits to a two-state exchange model. (B) Histogram showing the experimental $\Delta R_{2,eff} = R_{2,eff}(\nu_{CPMG\ 50\ Hz}) - R_{2,eff}(\nu_{CPMG\ 1000\ Hz})$ values for apo LgtC (red), apo LgtC-Q189E (green), and LgtC-Q189E-Gal (magenta) obtained using a 600 MHz spectrometer. The numbers are $\Delta R_{2,eff}$ values for residues with clipped histogram bars. Blanks indicate peaks with insufficient signal-to-noise ratios for reliable analysis.

the nucleotide phospho-sugar donor substrate and resembles the conformation of the resulting binary complex. In contrast, the "a" peaks correspond to a form of LgtC that is not directly competent for substrate binding.

We have speculated that the "a" and "b" conformations could perhaps differ by slow cis−trans isomerization of two proline residues in an active site loop that must at least transiently open to allow substrate binding and product release.[16] However, numerous alternative explanations can be envisioned, and it is important to reiterate that high-resolution structural information for apo LgtC is currently lacking. Also, the "a" and "b" peaks are reported by residues throughout the enzyme, and thus, the detected conformational changes, which remain to be structurally defined, are global rather than localized to its active site. Furthermore, the relative ratios of "a" to "b" peaks observed in both methyl-TROSY and ^{19}F-NMR spectra differ between individual residues (Figure 4 and Figure S4 of the Supporting Information). Although translating NMR peak intensities into populations is difficult because of possible differential relaxation effects, this suggests that the slowly interconverting "a" and "b" states may be conformationally heterogeneous. Therefore, we cannot conclude that the observed conformational exchange of LgtC on a time scale of seconds is strictly two-state.

The addition of the acceptor sugar lactose to form the ternary complex does not result in any further pronounced spectral changes relative to the UDP-2FGal·Mg^{2+} binary complex. However, the methyl-TROSY signals from two active site residues (Ile31 and Ile129) disappear upon lactose binding, suggestive of some additional conformational exchange.[16] Furthermore, the methyl signal from Ile191 exhibits the only clear chemical shift perturbation. Interestingly, this isoleucine is relatively distant from the bound substrates yet within the same helix has the two key "nucleophile candidates", Gln189 and Asp190. Thus, the NMR spectroscopic data may also reveal some subtle catalytically important conformational changes not observed in the essentially superimposable X-ray crystallographic structures of the LgtC binary and ternary complexes.[4]

LgtC Undergoes Conformational Interconversion on a Time Scale of Seconds. The time scale for interconversion of the two principal states of apo LgtC was determined from methyl-TROSY-detected magnetization transfer experiments. Because of limited spectral resolution, cross peaks linking the "a" and "b" signals were observed for only Ile31, Ile129, and an unassigned valine or leucine. However, this phenomenon, which qualitatively shows conformational exchange, is likely general for all residues in LgtC exhibiting multiple signals, as evidenced, for example, by weak cross-peaks in the ^{19}F-NOESY spectrum of the protein with CF_3Phe incorporated at position 132. In the case of Ile129, the data could be analyzed reliably to provide quantitative rate constants at 25 °C: $k_{a\rightarrow b} = 0.12 \pm 0.03$ s^{-1}, and $k_{b\rightarrow a} = 0.16 \pm 0.04$ s^{-1}. The mechanistic significance of this conformational equilibrium, on the time scale of seconds, is unclear for two reasons. First, it is too slow to be part of the catalytic cycle for the wild-type enzyme (k_{cat} = 46 s^{-1}), and second, nucleotide phospho-sugar donors bind to and thereby stabilize only the "b" state. Thus, without additional structural and functional information, the simplest conclusion from these studies is that the conformational excursions to the "a" state reduce the population of catalytically competent apo LgtC.

LgtC Also Exhibits Millisecond Time Scale Motions. Insights into faster millisecond time scale dynamic processes occurring in LgtC were provided by methyl relaxation

dx.doi.org/10.1021/bi301317d | *Biochemistry* 2013, 52, 320−332

dispersion experiments with selectively [^{1}H,^{13}C]Ile$^{\delta}$-labeled samples. Substantial conformational broadening on this time scale was observed for the both "a" and "b" signals of isoleucines throughout LgtC. These include residues in the active site (Ile76, Ile79, Ile104, and Ile191) as well as those more remote (Ile3, Ile31, and Ile129). Therefore, motions on this time scale are also global and superimposed on the slower "a" to "b" conformational equilibria. This indicates further that LgtC exhibits complex, multistate dynamics.

Somewhat unexpectedly, binding of UDP-2FGal·Mg^{2+} to LgtC alters but does not eliminate these millisecond exchange processes. Rather, within the limitations caused by the Mg^{2+}-induced aggregation of the binary complex and slow hydrolysis of the donor analogue, the bound "b" peaks for Ile104 actually showed an increased level of exchange broadening. This is particularly interesting because this active site isoleucine is the X residue in the Asp-X-Asp motif involved in metal binding.[4] Furthermore, these conformational exchange processes, with a k_{ex} of $\sim 10^3$ s^{-1}, are significantly faster than the k_{cat} of 46 s^{-1} for glycosyl transfer. Therefore, if indeed linked to catalysis, they may reflect prerequisite motions of the Michaelis complex necessary to establish a LgtC active site conformation that ultimately stabilizes the transition state for glycosyl transfer, via either an S_Ni-like or an S_N2 mechanism. Testing this rather speculative hypothesis will require additional studies, including those aimed at defining the conformations of the detected interconverting states.[31]

Dampened Motions in the Covalent Glycosyl–Enzyme Intermediate of LgtC-Q189E. In contrast to wild-type LgtC, the Q189E mutant forms an isolatable glycosyl–enzyme intermediate with Asp190 covalently modified by a galactosyl moiety.[10] To gain further insight into the substantial conformational change that must accompany this reaction, we also used NMR methods to characterize LgtC-Q189E. Although the ^{15}N-TROSY-HSQC spectra of this mutant showed many spectral perturbations relative to the spectrum of wild-type LgtC, their isoleucine methyl-TROSY spectra were for the most part superimposable. Given that main chain amides are generally more sensitive to structural and electrostatic perturbations than side chain methyl groups, and that a fraction of the LgtC-Q189E may be covalently modified from UDP-Gal present in the *E. coli* expression host, this implies that LgtC-Q189E retains a wild-type-like active site structure. Furthermore, relaxation dispersion measurements showed no dramatic differences in the millisecond time scale motions of its isoleucine methyl groups relative to those observed for wild-type apo LgtC. Therefore, within the limitations of these measurements, the Q189E mutation in LgtC does not lead to any obvious structural or millisecond dynamic changes that might account for its surprising propensity to form a glycosyl–enzyme intermediate via Asp190.

In contrast to apo LgtC-Q189E, the trapped glycosyl–enzyme intermediate showed a pronounced decrease in the methyl relaxation dispersion behavior of its isoleucine residues. This intermediate was enriched using a coupling enzyme system to deplete product UDP and confirmed by a 162 Da mass increase. The combination of the covalent linkage with a likely extensive network of hydrogen bonding and van der Waals contacts between the galatosyl moiety and LgtC could readily dampen motions over a range of time scales. Indeed, considerable evidence exists for suppression of dynamic behavior in trapped glycosyl–enzyme intermediates on glycoside hydrolases, including an increased level of protection from amide hydrogen exchange, decreased protease susceptibility, and resistance to thermal and chemical denaturation.[32,33] Interestingly, the k_{cat} value for galactosyl transfer by LgtC-Q189E is ~ 0.7 s^{-1}, which is on the same time scale seen for the slow global motions observed in the magnetization exchange experiments with the wild-type enzyme.[10] It is therefore feasible that the conformational changes required to place Asp190 into the correct position to capture the incipient oxocarbenium-like ion formed by the bound UDP-Gal in the active site of this mutant are those being observed with states "a" and "b" of the wild-type enzyme. Although speculative, these experiments show that exchange processes on such a time scale are certainly feasible.

In conclusion, we have discovered that the structural and dynamic properties of LgtC are far more complex than the simple active site loop motions suggested from the static X-ray crystallographic structures of its substrate complexes. The protein exists in multiple conformations that interconvert on a time scale of seconds, with each conformation also exhibiting millisecond motions. Nucleotide phospho-sugar donor substrates bind only to the "b" state of LgtC yet do not dampen these faster motions. However, formation of a glycosyl–enzyme intermediate in the Q189E mutant does restrict the flexibility of active site isoleucines. It is very likely that these complex conformational dynamics are shared by many glycosyltransferases, and defining the roles of such mobility in their catalytic functions and biological regulation will require several complementary experimental approaches. These approaches include kinetic studies to determine stepwise rate constants of binding and catalysis, the identification of mutations within active site regions, as well as at remote sites, that influence catalysis, and detailed NMR spectroscopic studies (spanning amide hydrogen exchange to relaxation dispersion and paramagnetic relaxation enhancement measurements) to characterize conformational dynamics along the pathway of glycosyl transfer.

■ ASSOCIATED CONTENT

Ⓢ Supporting Information

One table of kinetic data and seven figures, including proposed reaction mechanisms, the magnetization transfer pulse sequence and data analysis, and NMR and mass spectra of LgtC variants. This material is available free of charge via the Internet at http://pubs.acs.org.

■ AUTHOR INFORMATION

Corresponding Author

*Department of Biochemistry and Molecular Biology, Life Sciences Centre, University of British Columbia, Vancouver, BC V6T 1Z3, Canada. E-mail: mcintosh@chem.ubc.ca. Phone: (604) 822-3341. Fax: (604) 822-5227.

Funding

This research was supported by grants from the Natural Sciences and Engineering Research Council of Canada (L.P.M. and S.G.W.) and the Canadian Institutes for Health Research (S.G.W.). S.G.W. is the recipient of a Canada Research Chair in Chemical Biology.

Notes

The authors declare no competing financial interest.

■ ACKNOWLEDGMENTS

We thank Ryan Mehl (Franklin and Marshall College, Lancaster, PA) and Peter Schultz (The Scripps Research Institute, La Jolla, CA) for providing the tRNA/aminoacyl-tRNA synthetase plasmids used to incorporate unnatural amino acids into LgtC and Lewis Kay for NMR-related advice. Instrument support was provided by the Canadian Institutes for Health Research, the Canada Foundation for Innovation, the British Columbia Knowledge Development Fund, the University of British Columbia Blusson Fund, and the Michael Smith Foundation for Health Research.

■ ABBREVIATIONS

ESI-MS, electrospray ionization mass spectrometry; GT, glycosyltransferase; HSQC, heteronuclear single-quantum correlation; k_{cat}, catalytic rate constant; k_{cat}/K_m, apparent second-order rate constant; K_m, Michaelis constant; LgtC, lipopolysaccharide α-1,4-galactosyltransferase C; MALDI-TOF, matrix-assisted laser desorption ionization time-of-flight; NMR, nuclear magnetic resonance; pH*, pH meter reading without correction for isotope effects; TROSY, transverse relaxation optimized spectroscopy; UDP, uridine 5′-diphosphate; UDP-2FGal, uridine 5′-diphosphate 2-deoxy-2-fluorogalactose; UDP-Gal, uridine 5′-diphosphate galactose.

■ REFERENCES

(1) Cantarel, B. L., Coutinho, P. M., Rancurel, C., Bernard, T., Lombard, V., and Henrissat, B. (2009) The Carbohydrate-Active EnZymes database (CAZy): An expert resource for Glycogenomics. *Nucleic Acids Res. 37*, D233−D238.

(2) Moran, A. P., Prendergast, M. M., and Appelmelk, B. J. (1996) Molecular mimicry of host structures by bacterial lipopolysaccharides and its contribution to disease. *FEMS Immunol. Med. Microbiol. 16*, 105−115.

(3) Ly, H. D., Lougheed, B., Wakarchuk, W. W., and Withers, S. G. (2002) Mechanistic studies of a retaining α-galactosyltransferase from *Neisseria meningitidis*. *Biochemistry 41*, 5075−5085.

(4) Persson, K., Ly, H. D., Dieckelmann, M., Wakarchuk, W. W., Withers, S. G., and Strynadka, N. C. (2001) Crystal structure of the retaining galactosyltransferase LgtC from *Neisseria meningitidis* in complex with donor and acceptor sugar analogs. *Nat. Struct. Biol. 8*, 166−175.

(5) Snajdrova, L., Kulhanek, P., Imberty, A., and Koca, J. (2004) Molecular dynamics simulations of glycosyltransferase LgtC. *Carbohydr. Res. 339*, 995−1006.

(6) Chiu, C. P., Watts, A. G., Lairson, L. L., Gilbert, M., Lim, D., Wakarchuk, W. W., Withers, S. G., and Strynadka, N. C. (2004) Structural analysis of the sialyltransferase CstII from *Campylobacter jejuni* in complex with a substrate analog. *Nat. Struct. Mol. Biol. 11*, 163−170.

(7) Chiu, C. P., Lairson, L. L., Gilbert, M., Wakarchuk, W. W., Withers, S. G., and Strynadka, N. C. (2007) Structural analysis of the α-2,3-sialyltransferase Cst-I from *Campylobacter jejuni* in apo and substrate-analogue bound forms. *Biochemistry 46*, 7196−7204.

(8) Lougheed, B. (1998) *Neisseria meningitidis* lipopolysaccharide galactosyl transferase: Mechanistc investigations and applications for oligosaccharide synthesis. Ph.D. Thesis, Department of Chemistry, The University of British Columbia, Vancouver, BC.

(9) Lougheed, B., Ly, H. D., Wakarchuk, W. W., and Withers, S. G. (1999) Glycosyl fluorides can function as substrates for nucleotide phosphosugar-dependent glycosyltransferases. *J. Biol. Chem. 274*, 37717−37722.

(10) Lairson, L. L., Chiu, C. P., Ly, H. D., He, S., Wakarchuk, W. W., Strynadka, N. C., and Withers, S. G. (2004) Intermediate trapping on a mutant retaining α-galactosyltransferase identifies an unexpected aspartate residue. *J. Biol. Chem. 279*, 28339−28344.

(11) Lairson, L. L., Henrissat, B., Davies, G. J., and Withers, S. G. (2008) Glycosyltransferases: Structures, functions, and mechanisms. *Annu. Rev. Biochem. 77*, 521−555.

(12) Tvaroska, I. (2004) Molecular modeling insights into the catalytic mechanism of the retaining galactosyltransferase LgtC. *Carbohydr. Res. 339*, 1007−1014.

(13) Ardevol, A., and Rovira, C. (2011) The molecular mechanism of enzymatic glycosyl transfer with retention of configuration: Evidence for a short-lived oxocarbenium-like species. *Angew. Chem., Int. Ed. 50*, 10897−10901.

(14) Gómez, H., Polyak, I., Thiel, W., Lluch, J. M., and Masgrau, L. (2012) Retaining glycosyltransferase mechanism studied by QM/MM method: LgtC transfers α-galactose via an oxocarbenium ion-like transition state. *J. Am. Chem. Soc. 134*, 4743−4752.

(15) Lee, S. S., Hong, S. Y., Errey, J. C., Izumi, A., Davies, G. J., and Davis, B. G. (2011) Mechanistic evidence for a front-side, S_Ni-type reaction in a retaining glycosyltransferase. *Nat. Chem. Biol. 7*, 631−638.

(16) Chan, P. H. W., Weissbach, S., Okon, M., Withers, S. G., and McIntosh, L. P. (2012) NMR spectral assignments of α-galactosyltransferase LgtC from *Neisseria meningitidis*: Substrate binding and multiple conformational states. *Biochemistry 51*, 8278−8292.

(17) Kleckner, I. R., and Foster, M. P. (2011) An introduction to NMR-based approaches for measuring protein dynamics. *Biochim. Biophys. Acta 1814*, 942−968.

(18) Tugarinov, V., and Kay, L. E. (2003) Ile, Leu, and Val methyl assignments of the 723-residue malate synthase G using a new labeling strategy and novel NMR methods. *J. Am. Chem. Soc. 125*, 13868−13878.

(19) Tugarinov, V., Kanelis, V., and Kay, L. E. (2006) Isotope labeling strategies for the study of high-molecular-weight proteins by solution NMR spectroscopy. *Nat. Protoc. 1*, 749−754.

(20) Jackson, J. C., Hammill, J. T., and Mehl, R. A. (2007) Site-specific incorporation of a ^{19}F-amino acid into proteins as an NMR probe for characterizing protein structure and reactivity. *J. Am. Chem. Soc. 129*, 1160−1166.

(21) Cellitti, S. E., Jones, D. H., Lagpacan, L., Hao, X., Zhang, Q., Hu, H., Brittain, S. M., Brinker, A., Caldwell, J., Bursulaya, B., Spraggon, G., Brock, A., Ryu, Y., Uno, T., Schultz, P. G., and Geierstanger, B. H. (2008) In vivo incorporation of unnatural amino acids to probe structure, dynamics, and ligand binding in a large protein by nuclear magnetic resonance spectroscopy. *J. Am. Chem. Soc. 130*, 9268−9281.

(22) Delaglio, F., Grzesiek, S., Vuister, G. W., Zhu, G., Pfeifer, J., and Bax, A. (1995) NMRPipe: A multidimensional spectral processing system based on UNIX pipes. *J. Biomol. NMR 6*, 277−293.

(23) Goddard, T. D., and Kneeler, D. G. (1999) *Sparky 3*, University of California, San Francisco, CA.

(24) Sprangers, R., Gribun, A., Hwang, P. M., Houry, W. A., and Kay, L. E. (2005) Quantitative NMR spectroscopy of supramolecular complexes: Dynamic side pores in ClpP are important for product release. *Proc. Natl. Acad. Sci. U.S.A. 102*, 16678−16683.

(25) Sprangers, R., Velyvis, A., and Kay, L. E. (2007) Solution NMR of supramolecular complexes: Providing new insights into function. *Nat. Methods 4*, 697−703.

(26) Farrow, N. A., Zhang, O., Forman-Kay, J. D., and Kay, L. E. (1994) A heteronuclear correlation experiment for simultaneous determination of ^{15}N longitudinal decay and chemical exchange rates of systems in slow equilibrium. *J. Biomol. NMR 4*, 727−734.

(27) Korzhnev, D. M., Kloiber, K., Kanelis, V., Tugarinov, V., and Kay, L. E. (2004) Probing slow dynamics in high molecular weight proteins by methyl-TROSY NMR spectroscopy: Application to a 723-residue enzyme. *J. Am. Chem. Soc. 126*, 3964−3973.

(28) Kleckner, I. R., and Foster, M. P. (2012) GUARDD: User-friendly MATLAB software for rigorous analysis of CPMG RD NMR data. *J. Biomol. NMR 52*, 11−22.

(29) Liu, C. C., and Schultz, P. G. (2010) Adding new chemistries to the genetic code. *Annu. Rev. Biochem. 79*, 413−444.

(30) Jones, D. H., Cellitti, S. E., Hao, X., Zhang, Q., Jahnz, M., Summerer, D., Schultz, P. G., Uno, T., and Geierstanger, B. H. (2010)

Site-specific labeling of proteins with NMR-active unnatural amino acids. *J. Biomol. NMR 46*, 89−100.
(31) Baldwin, A. J., and Kay, L. E. (2009) NMR spectroscopy brings invisible protein states into focus. *Nat. Chem. Biol. 5*, 808−814.
(32) Connelly, G. P., Withers, S. G., and McIntosh, L. P. (2000) Analysis of the dynamic properties of *Bacillus circulans* xylanase upon formation of a covalent glycosyl-enzyme intermediate. *Protein Sci. 9*, 512−524.
(33) Poon, D. K., Ludwiczek, M. L., Schubert, M., Kwan, E. M., Withers, S. G., and McIntosh, L. P. (2007) NMR spectroscopic characterization of a β-(1,4)-glycosidase along its reaction pathway: Stabilization upon formation of the glycosyl-enzyme intermediate. *Biochemistry 46*, 1759−1770.